How Allosteric Effectors Can Bind to the Same Protein Residue and Produce Opposite Shifts in the Allosteric Equilibrium†

Donald J. Abraham,*,‡ Martin K. Safo,‡ Telih Boyiri,‡ Richmond E. Danso-Danquah,‡ Jean Kister,§ and Claude Poyart§

Department of Medicinal Chemistry, School of Pharmacy, Medical College of Virginia, Virginia Commonwealth University, Richmond, Virginia 23298-0540, and Physiologie et Physiopathologie Moléculaires du Globule Rouge, INSERM U299, 78, Rue du General Leclerc, 94275 Le Kremlin Bicêtre, France

Received February 24, 1995; Revised Manuscript Received June 27, 1995⊗

ABSTRACT: Monoaldehyde allosteric effectors of hemoglobin were designed, using molecular modeling software (GRID), to form a Schiff base adduct with the Val 1α N-terminal nitrogens and interact via a salt bridge with Arg 141α of the opposite subunit. The designed molecules were synthesized if not available. It was envisioned that the molecules, which are aldehyde acids, would produce a *high*-affinity hemoglobin with potential interest as antisickling agents similar to other aldehyde acids reported earlier. X-ray crystallographic analysis indicated that the aldehyde acids did bind as modeled de novo in symmetry-related pairs to the α subunit N-terminal nitrogens. However, oxygen equilibrium curves run on solutions obtained from T- (tense) state hemoglobin crystals of reacted effector molecules produced *low*-affinity hemoglobins. The shift in the allosteric equilibrium was opposite to that expected. We concluded that the observed shift in allosteric equilibrium was due to the acid group on the monoaldehyde aromatic ring that forms a salt bridge with the guanidinium ion of Arg 141 α on the opposite subunit. This added constraint to the T-state structure that ties two subunits across the molecular symmetry axis shifts the equilibrium further toward the T-state. We tested this idea by comparing aldehydes that form Schiff base interactions with the same Val 1α residues but do not interact across the dimer subunit symmetry axis (a new one in this study with no acid group and others that have had determined crystal structures). The latter aldehydes shift the allosteric equilibrium toward the R-state. A hypothesis to predict the direction in shift of the allosteric equilibrium is made and indicates that it is not exclusively where the molecule binds but how it interacts with the protein to stabilize or destabilize the T- (tense) allosteric state.

Hemoglobin (Hb)[1] has been the model system for investigating allosteric phenomena in proteins. It exists in two states: a relaxed (R) conformation when oxygenated and a tense (T) conformation in the deoxygenated state. The allosteric equilibrium can be shifted in either direction by allosteric effectors. When the allosteric equilibrium is shifted toward the R-state, a high-affinity Hb is obtained that more readily binds and holds oxygen while a shift toward the T-state produces the converse, a low-affinity hemoglobin that more easily releases oxygen. High-affinity hemoglobins exhibit a left shift, while low-affinity hemoglobins produce an opposite right shift in the oxygen equilibrium curve. Regulating the allosteric equilibrium in both directions has been of interest in medicine. Agents that produce a high-affinity Hb have been clinically evaluated as antisickling agents while those that produce a low-affinity Hb are being studied to treat diseases that arise from ischemia. Therefore, it has been of interest to understand the molecular details of the regulation of allosteric equilibria from both a theoretical and therapeutic point of view.

We have pondered a question for some time. Why do certain monocovalent acting allosteric effectors of Hb that bind to the same amino acid residue shift the allosteric equilibrium in opposite directions. For example, allosteric effectors such as 12C79, when incubated in air (when Hb is predominantly in the R-state conformation), bind to Val 1α and produce a high-affinity Hb (Beddell et al., 1984; Wireko & Abraham, 1991). On the other hand, we solved the structure of 4-carboxyphenyl isothiocyanate (4-CPI) several years ago (Wireko and Abraham, unpublished results) and found that it also binds to Val 1α when incubated in air yet produces a low-affinity Hb (Currell et al., 1982). Both 12C79 and 4-CPI contain an acid group and covalently bind to the same N-terminal amino group.

Our original intent in this study was to discover new allosteric effectors that improve on the antisickling characteristics of 12C79 (Beddell et al., 1984) and vanillin

† This work was supported in part by NIH HLBI Grant RO-1-32793 (to D.J.A.), Virginia Commonwealth University, and Institut National de la Santé et de la Recherche Médicale, la Fondation pour la Recherche Médicale, la Faculté de Médecine Paris-Sud et la Direction des Recherches, Etudes et Techniques.

* Address correspondence to this author.

‡ Virginia Commonwealth University.

§ INSERM.

⊗ Abstract published in *Advance ACS Abstracts,* September 1, 1995.

[1] Abbreviations: Hb, tetrameric human adult hemoglobin; 12C79 (formerly BW12C), 5-(2-formyl-3-hydroxyphenoxy)pentanoic acid; 4-CPI, 4-carboxyphenyl isothiocyanate (also referred in the literature reference as 4-isothiocyanatobenzoic acid); TLC, thin-layer chromatography; P_{50}, partial pressure at which 50% of the hemoglobin molecule is saturated with oxygen; n_{50}, the Hill coefficient at 50% hemoglobin saturation; 5-FSA, 5-formylsalicylic acid; 4-CBA, 4-carboxybenzaldehyde; MFSA, methyl 5-formyl-2-hydroxybenzoate; HMAB, methyl 2-hydroxy-5-acetalbenzoate; 5-FA, 5-formylaspirin; 2-BF, 2-(benzyloxy)-5-formylbenzoic acid; 2−4CBF, 2-(4-carboxybenzyloxy)-5-formylbenzoic acid; 2-PEF, 2-(phenylethyloxy)-5-formylbenzoic acid; DPG, 2,3-diphosphoglycerate; DMHB, 3,5-dimethyl-4-hydroxybenzaldehyde, K_T, equilibrium constant for the deoxy (T) state; L, allosteric equilibrium constant.

0006-2960/95/0434-15006$09.00/0

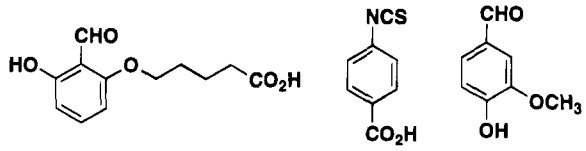

12C79 4-CPI vanillin

(Abraham et al., 1991). Both 12C79 and an analog had been under clinical investigation (Orringer et al., 1988), but the studies were discontinued. Vanillin left shifts the oxygen equilibrium curve like 12C79 but does not bind to Val 1α; it binds to two sites, one near Cys 104α, His 103α, and Gln 103β in the central water cavity and the other on the surface near His 116β and His 117β (Abraham et al., 1991). Vanillin has a very low toxicity profile and is currently in clinical trials. Therefore, our first goal was to design allosteric effectors that *increase* the oxygen affinity of hemoglobin. We targeted reaction at Val 1α with monoaldehyde acids (like 12C79) that would contain the low-toxicity profile of vanillin and aspirin (salicylate aldehydes). To our surprise all but one of the new effectors *decreased* the oxygen affinity of hemoglobin. These unexpected results shifted our attention away from drug discovery toward studies aimed at establishing a molecular understanding for the regulation of the allosteric equilibrium in either direction.

MATERIALS AND METHODS

Materials and General Procedures. All reagents used in the synthesis were purchased from Aldrich Chemical Co., Lancaster, Kodak, and Fluka. All reagents were used directly as the starting materials without purification. Solvents were purchased from Fisher Scientific Co. and Aldrich Chemical Co. The solvents, methanol and acetone, were purchased as HPLC grade and were used without purification. THF was dried over lithium aluminum hydride and then distilled.

Silica gel coated plates (0.25 mm thickness) were purchased from Analtech Inc. and used for thin-layer chromatography (TLC). The separations were spotted by visualizing under UV light (254 nm), iodine chamber, or Dragendorff's reagent. Flash chromatographic separations were done using Merck, grade 9385, 230−400 mesh, 60 Å silica gel.

The proton magnetic resonance (^{1}H NMR) spectra were recorded on a GE 300 MHz spectrometer and are reported in parts per million (δ ppm) with tetramethylsilane (TMS) as an internal standard. Elemental analyses were conducted at Atlantic Microlab, Inc., in Norcross, GA, and are within 0.4% of the calculated values. Intermediate compounds were analyzed by TLC and ^{1}H NMR but are not reported. Melting points (mp) were determined on a Thomas-Hoover capillary melting point apparatus and are uncorrected.

HbA was generously provided by Drs. John Hess and Victor MacDonald of the U.S. Army Medical Research Detachment, formerly based at the Letterman Laboratories, The Presidio, San Francisco, CA. For oxygen dissociation analyses, HbA was further purified by dialysis against pH 8.6 Tris buffer (50 mM, containing 40 mg of EDTA/L) to remove any residual A2 hemoglobin. The pure adult Hb fraction (HbA) was concentrated using a Schleicher and Schuell collodion bag apparatus (Schleicher and Schuell Inc.) with HEPES buffer (50 mM, pH 7.4) as the exchange buffer. The Hb concentration at this point was usually found to be around 35 g % (approximately 5.4 mM) with less than 5% methemoglobin. For all other experiments HbA was dialyzed against 10 mM phosphate buffer, pH 7.0. The concentration of HbA at this time was normally 2 mM. All purified hemoglobin solutions were stored at −82 °C until ready for use. The reagents and buffers were purchased from Sigma Chemical Co., Fisher Scientific Co., and Pharmacia and Research Chemicals, Inc.

Molecular Modeling. GRID is a computational procedure for mapping energetically favorable binding sites on macromolecules of known structure (Goodford, 1985). The interaction of specific probe groups with the target macromolecule structure is estimated using electrostatic, hydrogen bond, and Lennard-Jones energy calculations:

$$E_{xyz} = \sum E_{ij} + \sum E_{el} + \sum E_{hb}$$

where E_{ij} is the Lennard-Jones function, E_{el} is the electrostatics function, and E_{hb} is the hydrogen bond function. The energy levels (indicating an attraction between probe and macromolecule target) are contoured for each probe and displayed by computer graphics together with the target structure. In this study we employed GRID to model Hb near the α subunit N-terminal nitrogen atoms for potential binding interactions of the Schiff base adducts. The Hb 1.7 Å T-state atomic coordinates (Fermi et al, 1984) were used for the target molecule. Carboxylate and hydroxide probes were employed first since these are the key functional groups on the salicylates and vanillin. Other probes that were used include a methylene group, a methyl group, and an aromatic carbon. The energy of interaction between the probes and the target was contoured for display on an Evans and Sutherland Graphic System (PS 390). The carboxylate probe exhibited the highest contours in the GRID map near the two Arg 141α side chains. The hydroxide and carboxylate probes produced significant contours near the α subunit Ser 131, Ser 138, Lys 127, and Thr134 residues. The methylene, methyl, and aromatic probes also resulted in contours near Ala 130α. The aldehyde molecule was then fit into the map so that the aldehyde's functional groups (carboxylate and the phenoxy oxygen) would superimpose on the corresponding density for that functional group. In the case of 5-FSA, two possible orientations for the monoaldehyde could be fit to the GRID probe sites for carboxylate and hydroxyl (see Results).

Oxygen Dissociation Curves. In Paris, T-state crystals of reacted and reduced allosteric effector−Hb complexes were dissolved in 100 mM NaCl and bis-Tris buffer, pH 7.2. Measurements of the oxygen dissociation curves were performed using a Hemox analyzer (TCS Medical products) as described in detail previously (Abraham et al., 1992b; Kister et al., 1987). The P_{50} and n_{50} values were calculated by linear regression analysis from data points comprised between 40% and 60% oxygen saturation. The composition of the buffer system was 100 mM NaCl and 50 mM bis-Tris buffer at pH 7.2 at 25 °C. Catalase (20 μg/mL) and 50 μM EDTA were added to limit oxidation of the hemes during the 45−60 min of the recordings.

Reaction Conditions. Reaction of the monoaldehyde compounds with HbA followed the procedures of Wireko and Abraham (1991) with some slight modifications. Freshly prepared solutions of the compounds in 50 mM potassium phosphate buffer, pH 7.2, were incubated with oxy-HbA (dialyzed in 10 mM phosphate buffer, pH 7.0) tetramer/compound molar ratios of 1:5 or 1:10 for at least 24 h. Sodium cyanoborohydride in 50 mM phosphate buffer, pH 7.2, was added in 10−50-fold molar excess of the HbA

Table 1: Crystallographic Data

compd added to HbA	[compd]/[HbA]	cell dimensions				d_{lim},[a] Å	R_{int} or R_{merge},[b] %	R_{d-n},[c] %
		a, Å	*b*, Å	*c*, Å	β, deg			
5-FSA[d,f]	5	63.20	83.48	53.83	99.57	1.94	5.9	10.4
5-FSA[d,g]	5	63.21	83.46	53.80	99.42	1.94	5.2	8.0
4-CBA[e,f]	5	63.26	83.65	53.78	99.88	4.0	6.0	9.5
5-FA[d,f]	5	63.25	83.60	53.79	99.40	1.94	6.6	11.0
2-BF[d,f]	10	63.16	83.44	53.97	99.44	1.94	6.7	12.5
2-PEF[d,f]	5	63.31	83.61	53.86	99.39	1.94	5.4	11.6
2-4CBF[d,f]	5	63.38	83.64	53.86	99.44	1.94	5.6	11.2
DMHB[d,f]	5	63.34	83.71	53.85	99.33	1.94	5.1	10.2

[a] d_{lim} is the radius of the limiting sphere in which data were collected. [b] R_{int} is the agreement factor of intensities between Friedel pairs within each set of diffractometer data; $R_{int} = \sum_{hkl}(|I_{hkl}| - I_{hkl}|)/\sum_{hkl}(I_{hkl})$. R_{merge} is the consistency of equivalent reflections between the entire R-axis IIC image plate data set; $R_{merge} = \sum\sum|F^2(I)/G(I) - \langle F^2(h)\rangle|/\sum\sum F^2(I)/G(I)$. [c] R_{d-n} is the agreement factor of structure amplitudes between native and derivative data; $R_{d-n} = \sum_{hkl}(|F_d| - |F_n|)/\sum_{hkl}|F_d|$. [d] Data set from R-axis IIC image plate. [e] Data set from diffractometer. [f] Data set from crystals obtained from incubation and reduction of the aldehydic compounds and HbA in air. [g] Data set from crystals obtained from incubation and reduction of the aldehydic compounds and HbA under anaerobic condition.

tetramer to reduce the Schiff base adduct for at least 3 h. Purification was made by crystallization. The derivatized hemoglobin crystals were characterized by dissolution of the crystals and sequencing (as shown below). Isoelectric focusing electrophoresis for two of the crystals, 2-BF and DMHB, was also run at 4 °C.

Crystallization and X-ray Data Collection. Crystallization and X-ray data collection of the deoxygenated HbA−compound complexes followed the procedures of Perutz (1968) and Wireko and Abraham (1991) with some minor modifications. X-ray quality crystals for all complexes were obtained after 3−7 days. Crystals of 5-formylsalicylic acid (5-FSA), 4-carboxybenzaldehyde (4-CBA), 5-formylaspirin (5-FA), 2-(benzyloxy)-5-formylbenzoic acid (2-BF), 2-(phenylethyloxy)-5-formylbenzoic acid (2-PEF), 2-(4-carboxybenzyloxy)-5-formylbenzoic acid (2−4CBF), and 3,5-dimethyl-4-hydroxybenzaldehyde (DMHB) complexes that were grown from solutions of HbA incubated and reduced under *oxy* conditions were used for data collection. Crystals of 5-FSA for data collection were also grown from solutions of HbA incubated under *deoxy* conditions and then reduced. This experiment was designed to see if any binding preference for the same aldehyde is shown by incubation under oxy vs deoxy conditions.

X-ray diffraction data for the HbA−4-CBA complex were collected using a Rigaku RU-200 rotating anode and an AFC5R diffractometer to a resolution of 3.0 Å. All $hk\pm l$ reflections and their Friedel pairs were collected. One crystal, with dimensions between 0.3 and 0.8 mm, was used for the data collection. Diffraction data for the rest of the complexes were collected with a Rigaku RU-200 rotating anode generator equipped with an R-axis IIC image plate system, all to a resolution of 1.94 Å. Crystals of linear dimensions 0.2−0.5 mm were used. Crystallographic data are summarized in Table 1.

Difference Map Calculations. Raw data sets were processed as described (Wireko & Abraham, 1991) or with the Rigaku R-axis II software programs (Molecular Structure Corp., Dallas, TX). Difference electron density maps were computed from $[F_{obs(deriv)} - F_{obs(native)}]$ amplitudes at 4.0, 3.5, 3.0, and 2.0 Å resolution, where $F_{obs(deriv)}$ are the observed structure factors from the previously determined structure of native T-state Hb (Fermi et al., 1984). The difference map for 4-CBA was only calculated at 4.0 Å. Electron density maps from all four resolutions produced similar results with overlapping contours for the primary binding sites. The higher the resolution, the noisier the map, with the 2.0 Å map the most noisy. The structure amplitude agreement factors between native and derivative data (R_{d-n}) are reported in Table 1 at 2.0 Å resolution except for 4-CBA (4.0 Å). The maps were contoured at 3.0−4.0σ, where σ is the rms electron density in the unit cell. $[2F_{obs(deriv)} - F_{obs(native)}]$ maps were also calculated at the above resolutions and contoured at 1.0σ to confirm the drug positions. Models of the compounds created with MMOD12 (Still et al., 1989) and minimized with MM2 force field were fit to the electron density by using FRODO (Evans, 1985) on an Evans and Sutherland PS390 graphic station. All maps were fit at each stage of analysis (4.0, 3.5, 3.0, and 2.0 Å) with no apparent differences in density distribution at the observed binding sites. Figure 2 illustrates the difference electron density maps for four of the bound monoaldehydes (5-FSA, 2-BF, 2-PEF, DMHB). All binding site contours, and those associated with movement of residues near the binding sites, appeared as the highest peaks, well above any other density.[2] The 2.0 Å refined structures (with and without the addition of oxygen to the T-state crystals) will be published separately.

Sequencing. The sequencing experiments were run by Commonwealth Biotechnologies Inc., Richmond, VA 23219, using a Hewlett-Packard G1005A protein sequencer. Single crystals of derivatized T-state hemoglobin selected from the batches used for X-ray studies were dissolved in approximately 200 μL of doubly distilled water. For each sample, 50 μL was diluted 1:1 in 0.2% (v/v) trifluoroacetic acid in water and the entire sample applied to a prepared sequencing cartridge. Automated sequence analysis was done on five cycles for each sample; the picomoles of each PTH-amino acid detected was tabulated to determine cycle yields. The secondary amine produced by the reduction of the Schiff base double bond appears to produce a new PTH-amino acid derivative with different retention times than the standard PTH-amino acid peaks. The remainder of the α and β chains sequenced in the normal ratios expected for the two different subunits. The average chain sequencing was calculated from a comparison of the predicted first cycle yield of Val based on the average of the picomole yields of His_β (second cycle), Leu_β (third cycle), and Ala_α (fifth cycle).

Synthesis. (A) Methyl 5-Formyl-2-hydroxybenzoate (MFSA). A solution of 5-formylsalicylic acid (5-FSA) (5.0 g, 30 mmol) and concentrated sulfuric acid (4 mL, 71 mmol) in methanol (50 mL) was refluxed for 24 h. The reaction mixture was cooled and evaporated to dryness under reduced pressure. The residual product was dissolved in ethyl acetate and washed thoroughly with an aqueous solution of sodium bicarbonate. The organic layer was dried ($MgSO_4$) and evaporated to dryness to give a pale yellow solid: yield 4.97 g (92%); mp 72−74 °C; ^{1}H NMR (DMSO-d_6) δ 9.91 (s, 1H, CHO), 8.39 (d, J = 4.2 Hz, 1H, ArH), 8.0 (dd, J = 4.2, 8.4 Hz, 1H, ArH), 7.1 (d, J = 8.4 Hz, 1H, ArH), 4.02 (s, 3H, OCH_3). Anal. Calcd for $C_9H_8O_4$: C, 60.00; H, 4.47. Found: C, 60.05; H, 4.46.

(B) Methyl 2-Hydroxy-5-acetalbenzoate (HMAB). Methyl 5-formyl-2-hydroxybenzoate (MFSA) (4.0 g, 22 mmol),

[2] Coordinates for reported structures in this paper can be obtained from the corresponding author.

ethylene glycol (12 mL, 88 mmol), *p*-toluenesulfonic acid monohydrate (1.20 g), and toluene (100 mL) were charged into a round bottom flask fit with a Dean Stark apparatus and refluxed for 12 h with continuous removal of water. The reaction mixture was cooled and washed with an aqueous solution of sodium bicarbonate; the organic layer was dried ($MgSO_4$) and evaporated under reduced pressure. Flash chromatography using hexane/ethyl acetate (3:1) mixtures as eluant gave a brown viscous liquid as the product: yield 4.34 g (88%); ^{1}H NMR (DMSO-d_6) δ 10.65 (br s, 1H, OH), 7.89 (d, J = 4.1 Hz, 1H, ArH), 7.59 (dd, J = 4.1, 8.2 Hz, 1H, ArH), 7.01 (d, J = 8.2 Hz, 1H, ArH), 5.7 (s, 1H, CH), 3.92−4.1 (m, 4H, CH_2CH_2), 3.9 (s, 3H, OCH_3). Anal. Calcd for $C_{11}H_{12}O_5$: C, 58.89; H, 5.41. Found: C, 59.04; H, 5.55.

(C) 5-Formylaspirin (5-FA). 5-Formylsalicylic acid (5-FSA) (3.2 g, 20 mmol), acetyl chloride (1.88 g, 20 mmol), and triethylamine (4.08 g, 40 mmol) in 50 mL of dry ethyl ether were stirred at room temperature for 5 h. The reaction mixture was extracted with cold dilute aqueous HCl (0.1 M), and the ether layer was washed with cold water and brine, dried over anhydrous $MgSO_4$, and filtered. Petroleum ether was added, and the product crystallized out of solution at 4 °C: yield 2.91 g (70%); mp 115 °C; ^{1}H NMR (DMSO-d_6) δ 10.02 (s, 1H, CHO), 8.06 (d, J = 4.1 Hz, 1H, ArH), 7.49 (dd, J = 4.1, 8.2 Hz, 1H, ArH), 7.25 (d, J = 8.2 Hz, 1H, ArH), 2.30 (s, 3H, CH_3). Anal. Calcd for $C_{10}H_8O_5$: C, 57.69; H, 3.87. Found: C, 57.88; H, 3.88.

(D) 2-(Benzyloxy)-5-formylbenzoic Acid (2-BF). Methyl 2-hydroxy-5-acetalbenzoate (HMAB, 1.0 g, 4.46 mmol), benzyl bromide (0.76 g, 4.46 mmol), and powdered potassium carbonate (2.0 g, 14.5 mmol) in dry acetone were refluxed for 12 h. The reaction mixture was filtered and the solvent was removed under vacuum. The crude product was dissolved in ethyl acetate and washed with aqueous sodium hydroxide, dried ($MgSO_4$), and evaporated *in vacuo* to give the intermediate, methyl 2-(benzyloxy)-5-acetalbenzoate, as a colorless solid. A mixture of methyl 2-(benzyloxy)-5-acetalbenzoate and 10% aqueous potassium hydroxide (20 mL) was refluxed for 1 h, filtered, cooled, and acidified with concentrated hydrochloric acid. The precipitate was filtered and washed thoroughly with water (100 mL) and then diethyl ether. Air-drying yielded 1.01 g (88%) of product: mp 105−107 °C; ^{1}H NMR (DMSO-d_6) δ 9.91 (s, 1H, CHO), 7.2−8.6 (m, 8H, ArH), 5.35 (s, 2H, CH_2). Anal. Calcd for $C_{15}H_{12}O_4$: C, 70.34; H, 4.72. Found: C, 70.17; H, 4.99.

(E) 2-(4-Carboxybenzyloxy)-5-formylbenzoic Acid (2-4CBF). Methyl 2-hydroxy-5-acetalbenzoate (HMAB) (1.0 g, 4.46 mmol), methyl 4-(bromomethyl)benzoate (1.02 g, 4.46 mmol), and powdered potassium carbonate (2.0 g, 14.5 mmol) in dry 2-butanone were refluxed for 10 h. The reaction mixture was filtered while hot, and the solvent was removed under vacuum. The crude material was dissolved in ethyl acetate, washed with aqueous sodium hydroxide (0.5 M), dried ($MgSO_4$), and evaporated under reduced pressure to give a solid intermediate diester. The diester in 10% aqueous potassium hydroxide (30 mL) was refluxed for 1 h, filtered, cooled, and acidified with concentrated hydrochloric acid. The precipitate was filtered and washed thoroughly with water (100 mL) and then with small amounts of diethyl ether. Air-drying of the solid material yielded 1.21 g (90%): mp 215 °C; ^{1}H NMR (DMSO-d_6) δ 9.91 (s, 1H, CHO), 8.39 (d, J = 4.1 Hz, 1H, ArH), 7.9−8.06 (m, 3H, ArH), 7.45 (d, J = 8.9 Hz, 2H, ArH), 7.15 (d, J = 8.2 Hz, 1H, ArH), 4.5 (s, 2H, CH_2). Anal. Calcd for $C_{16}H_{12}O_6 \cdot 1.5H_2O$: C, 59.54; H, 4.53. Found: C, 59.82; H, 4.23.

(F) 2-(Phenylethyloxy)-5-formylbenzoic Acid (2-PEF). Methyl 2-hydroxy-5-acetalbenzoate (HMAB) (1.0 g, 4.46 mmol), 2-phenylethyl bromide (0.98 g, 5.27 mmol), and powdered potassium carbonate (2.0 g, 14.5 mmol) in dry acetone were refluxed for 12 h. The reaction mixture was filtered while hot, and the solvent was removed under vacuum. The crude product was dissolved in ethyl acetate, washed with aqueous sodium hydroxide (0.5 M), dried ($MgSO_4$), and evaporated under reduced pressure to give a solid intermediate, methyl 2-(phenylethyloxy)-5-acetalbenzoate, as a colorless material. Methyl 2-(phenylethyloxy)-5-acetalbenzoate was stirred in 10% aqueous potassium hydroxide (20 mL) and refluxed for 1 h; the reaction mixture was filtered, cooled, and acidified with concentrated hydrochloric acid. The precipitate was filtered and washed thoroughly with water (100 mL) and then with small amounts of diethyl ether. Air-drying of the solid material yielded 0.96 g (80%): mp 112−114 °C; ^{1}H NMR (DMSO-d_6) δ 13.05 (s, 1H, CO_2H), 9.92 (s, 1H, CHO), 8.19 (d, 1H, ArH), 8.01 (dd, J = 4.1, 8.2 Hz, 1H, ArH), 7.2−7.45 (m, 6H, ArH), 4.35 (t, J = 6.1 Hz, 2H, CH_2), 3.05 (t, J = 6.1 Hz, 2H, CH_2). Anal. Calcd for $C_{16}H_{12}O_4 \cdot 0.25H_2O$: C, 69.94; H, 5.32. Found: C, 70.29; H, 5.28.

RESULTS

Design. The design of new allosteric effectors was focused around the N-terminal amino groups of the α chains since they are primarily unprotonated at physiological pH; they are the most likely nucleophiles on the protein to form Schiff base interactions with aldehydes. The N-terminal amino groups of the β chains are not as readily accessible for reaction when the aldehydes are incubated in air (oxy-Hb); the opening of the β cleft at the N-terminal nitrogens is narrowed in oxy-Hb, and it has been shown that the natural allosteric effector 2,3-diphosphoglycerate (DPG) does not bind well to oxy-Hb (Benesch et al., 1968).

The molecular modeling program GRID (Goodford, 1985) was employed to model the region near the α-subunit N-terminal nitrogen atoms for additional binding interactions once the Schiff base has formed. GRID utilizes atom or group probes to identify complementary binding interactions. Carboxylate and hydroxide probes were first employed since these are the key functional groups on the salicylates and vanillin. GRID identified potential hydrogen bond or salt interactions with Ser 131, Ser 138, Thr 134, and Arg 141α in deoxy-Hb. Two monoaldehyde molecules that contain carboxyl and/or phenolic hydroxyl groups were fit into the GRID sites, 5-formylsalicylic acid (5-FSA) and 4-carboxybenzaldehyde (4-CBA).

(A) Salicylate Analogs. Two suitable binding modes for 5-FSA were consistent with the GRID map (Figure 1). In the first, the aldehyde forms a Schiff base linkage with the α subunit N-terminal amino group while the carboxylate forms a salt bridge with the Arg 141 guanidinium group of the other α subunit (Figure 1a). In the second binding mode, the aldehyde is bound to the N-terminal amino groups of the α subunits while the carboxylate forms a network of hydrogen bonds with the Ser 131, Ser 138, and Thr 134 side-chain hydroxyl groups of the same α chain (Figure 1b). The conformation observed in Figure 1a, involving a salt bridge

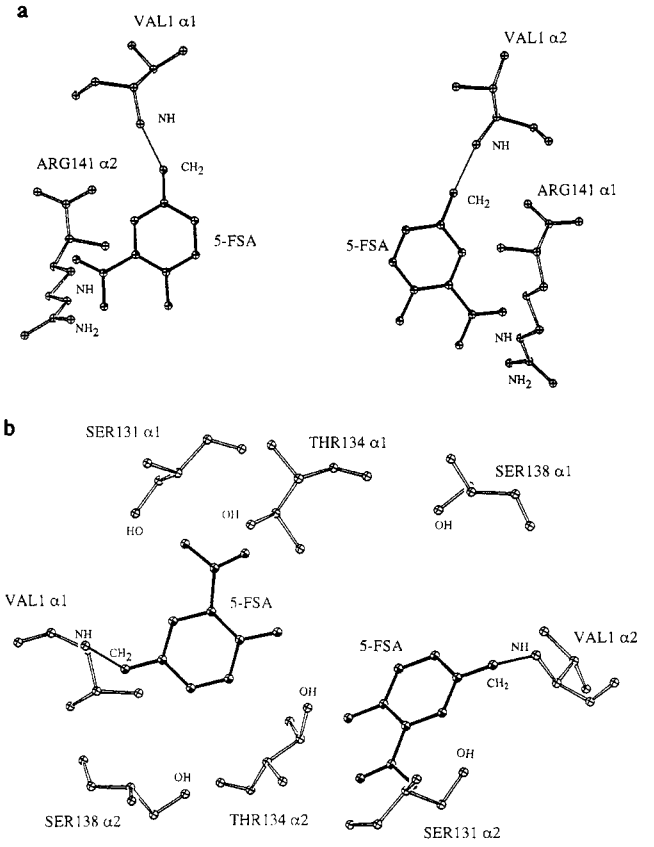

FIGURE 1: Two suitable binding modes for 5-FSA consistent with the GRID map. (a) The aldehyde forms a Schiff base linkage with the α subunit N-terminal amino group while the carboxylate forms a salt bridge with the Arg 141 guanidinium group of the other α subunit. (b) The aldehydes are bound to the N-terminal amino groups of the α subunits while the carboxylate forms a network of hydrogen bonds with the Ser 131, Ser 138, and Thr 134 side-chain hydroxyl groups of the same α chain.

with Arg 141α, was predicted as the preferred binding orientation because of the stronger salt bridge interaction; the guanidinium ion of Arg 141 α has also been shown to form an important salt bridge with the acid group of noncovalent-acting allosteric effectors (Wireko et al., 1991; Abraham et al., 1992b).

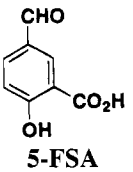

5-FSA

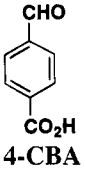

4-CBA

4-CBA differs from 5-FSA by removal of the *p*-hydroxyl group with a shift of the carboxyl group to the *para* position. The position of the acid group *para* to the aldehyde only permitted interaction of one carboxylate oxygen with the guanidinium group of Arg 141α. No other placements for 4-CBA were found to be as good.

Using the coordinate positions obtained for 5-FSA, the 5-FSA *p*-hydroxyl group was replaced with three different ether linkages: benzyloxy (2-BF), phenylethyloxy (2-PEF), and 4-carboxybenzyloxy (2−4CBF). Molecular modeling showed that the additional phenyl rings as well as the carboxyl group of 2−4CBF extended toward the ammonium ion of Lys 99α deeper in the central water cavity.

(B) 3,5-Dimethyl-4-hydroxybenzaldehyde. 3,5-Dimethyl-4-hydroxylbenzaldehyde (DMHB) is an aldehyde that contains two methyl groups that flank a phenolic hydroxyl group. It should also form a Schiff base with the N-terminal α-amino groups. DMHB was selected for study to evaluate the steric effects of the methyl groups that should hinder the phenol hydroxyl from interaction with the protein. Also, DMHB does not contain an acid group that would orient the aromatic ring toward Arg 141α on the opposite α chain. Therefore, we anticipated that this aldehyde might be oriented differently than the others.

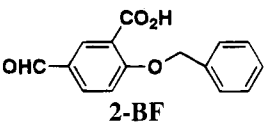

2-BF

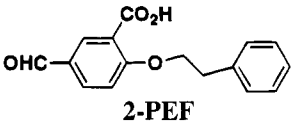

2-PEF

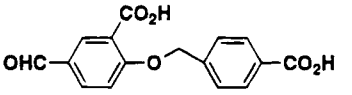

2-4CBF

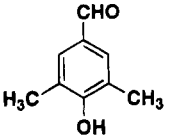

DMHB

Synthesis. The monoaldehydes that were synthesized are indicated in Scheme 1. The synthesis employed standard organic reactions.

Characterization of Crystals Used for the Diffraction Studies: Sequencing. Excess allosteric effector was incubated and reduced to assure complete reaction of the N-terminal Val nitrogens of the α chains (see Materials and Methods). The incubations and reductions were performed in air (when Hb is predominantly in the *R* conformation) for all effectors. 5-FSA was also incubated and reduced under deoxygenated (T-state) conditions. Crystallization was the primary method of purification (see below).

Automated Edman sequence analysis was performed on solutions made from crystals of two of the reduced monoaldehydes (DMHB and 5-FSA) to determine how many Val 1 (α and β) residues were reacted. The first five residues of each chain in the Hb dimer were sequenced. It was assumed that if the N-terminal Val 1 amino groups were reacted to form a Schiff base, the Edman degradation would not form a phenylthiohydantoin (PTH) derivative, and the chain sequencing reaction would terminate. Reduced levels of the Val 1-PTH derivative were observed (as expected from the Schiff base formation); however, normal levels of the PTH derivatives that correspond to the next four residues of each chain were found. Further consideration of the basic Edman reaction led us to conclude that the secondary amine that results from the reduction of the Schiff base linkage is also a suitable nucleophile that can form a new PTH derivative that would not match the PTH retention times for the 20 natural amino acids. This idea was tested using two synthetic peptides purified by conventional tBOC chemistry protocols (VHLGPA-NH_2 and LGHPVA-NH_2). Both peptides were reacted with representative aldehydes and reduced under identical reaction conditions used for hemoglobin. The products were then subjected to automated sequence analysis. The results clearly showed that both peptides produced novel PTH adducts while the remaining residues sequenced normally. Therefore, we postulate that PTH formation from

Scheme 1

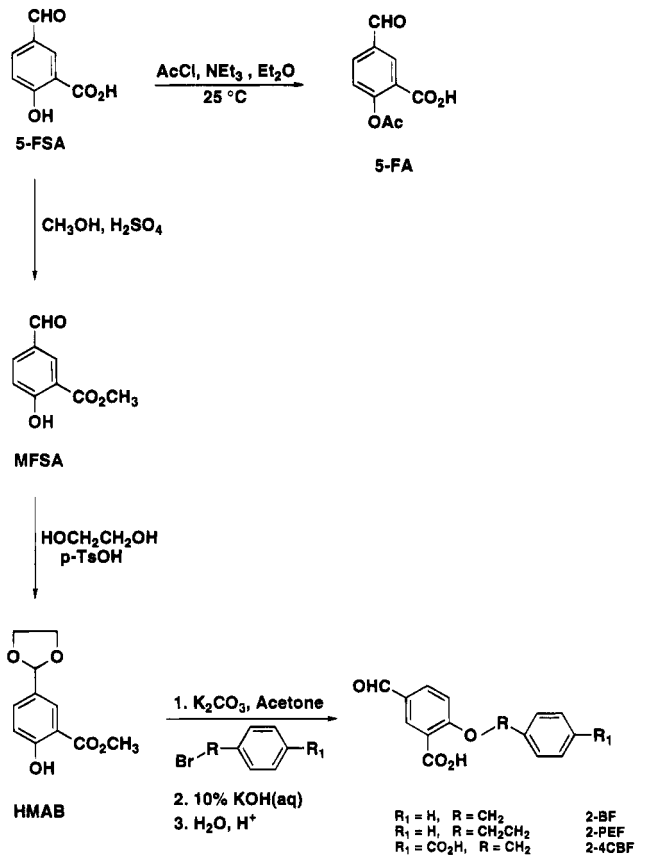

the reduced aldehyde adducts proceeds through a similar mechanism as found for proline, an imino acid. These results will be published separately (R. Harris, T. Boyiri, and D. J. Abraham, unpublished results).

The number of N-terminal Val 1 amino residues reacted was estimated by comparing the concentration (pmol) of Val-PTH observed vs what would be found if all Val residues were unreacted. The amount of unreacted Val was determined from the average of the picomole concentrations for Ala α5-, His β2-, and Leu β3-PTH derivatives; i.e., 1 Val-PTH = average/2. For DMHB the amount of Val-PTH observed was 2296 pmol, and the equivalent for one Val would be 1082 pmol. This gives a ratio of 2296/1082 or 2.12 Val that were not derivatized and 1.88 residues that had reacted to form a Schiff base. This is in agreement with the results of the crystal structure discussed below showing exclusive binding to the two Val 1α residues. Likewise, the 5-FSA (that was incubated under deoxy conditions then reduced), 345 pmol of the Val-PTH derivative was observed, and the equivalent for one Val was 457 pmol. Hence less than one Val (0.75) residue is not reacted. This again agrees with the X-ray crystal structure determination below that shows that both α and β chains were reacted with the predominant reaction at the α chains.

Difference Electron Density Maps/Isoelectric Focusing Electrophoresis. X-ray diffraction of protein crystals containing bound molecules produces a composite picture of any primary and secondary binding sites (and their relative occupancies) when these sites appear as the highest density in the difference electron density maps (as found in these studies). Difference electron density maps are very sensitive in determining ordered binding above 10−20% occupancy. In general, the crystal lattice will not permit significant amounts of nonspecific binding (especially on the surface) without distortion of the crystal and loss of isomorphous properties. We have observed this previously by increasing the amount of allosteric effector to observe the limit of the number of binding sites (Abraham et al., 1983).

The number of binding sites observed in the X-ray maps and those indicated by sequencing (i.e., reaction at the β1 Val residues) was further characterized by comparison with the number of bands observed by electrophoresis on solutions obtained from crystals used to do the structural analysis.

Two crystals were chosen for isoelectric focusing electrophoresis, one representing exclusive binding in the difference maps (DMHB) and one representing the highest degree of multiple binding sites in the difference maps (2-BF). The DMHB electrophoresis gave a simple pattern (one major reaction band and a smaller band indicating unreacted Hb <15%) as would be expected for primary binding to Val 1α as observed crystallographically and supported by sequencing. Two very small satellite bands (total estimated at <5%) might represent some binding at the Val 1β termini or Lys residues such as Lys 99α.

2-BF showed a more complex pattern as expected from multiple binding sites observed in the X-ray maps and the sequencing experiments that showed three of the four N-termini reacted. Additional binding sites for 2-BF in the difference density maps were found with two different conformations at Lys 99α with approximately 30% relative occupancy to the primary peaks at Val 1α (see X-ray results). The isoelectric focusing electrophoresis showed two major bands and two secondary bands with some unreacted Hb (estimated around 10%). This pattern is most likely related to the following products identified by difference maps and sequencing: Val 1α-unreacted-Val 1β-unreacted-Lys 99α-unreacted, i.e., unreacted Hb; Val 1α-reacted-Val 1β-unreacted-Lys 99α-unreacted; Val 1α-reacted-Val 1β reacted-Lys 99α-unreacted; and Val 1α-reacted-Val 1β-reacted-Lys 99α-reacted. From this study and the one in the accompanying paper (Boyiri et al., 1995) on the comparison of the electrophoresis patterns with difference electron density maps and the sequencing experiments, the X-ray difference maps appear to give a very good first-order indication of the primary binding sites.

X-ray Crystallography. (A) 5-Formylsalicylic Acid (5-FSA). The results of the 5-FSA crystal structure (Figure 2a) confirmed the predicted binding site determined by the modeling experiments (Figure 1a). The 5-FSA carboxylate interaction with Arg 141α orients the *para*-substituted hydroxyl of the aromatic ring diagonally down the central water cavity toward Lys 99α. Close contacts with the protein are shown in Figure 3a. The hydroxide of the 5-FSA interacts with the side-chain hydroxyl of Thr 134α. The shortest contact (3.0 Å) involves the β carbon of Ala 130α with the phenol oxygen of 5-FSA. There are positive and/or negative peaks found on or around the following globin residues: Val 1α, Arg 141α, Thr 134α, Lys 127α, Ala 130α, and Ser 131α, indicating minor Hb residue movements. The position of the acid group on the aromatic ring appears to play a role in orienting the molecule after binding to theN-terminal amino groups of the α chains. A secondary binding site was observed, with about 10% relative occupancy to the primary site, at the β_1 N-terminal amino group. The symmetry-related binding on the β_2 subunit N-terminal nitrogen is lower. No attempt was made to fit the 5-FSA molecule at the two β sites.

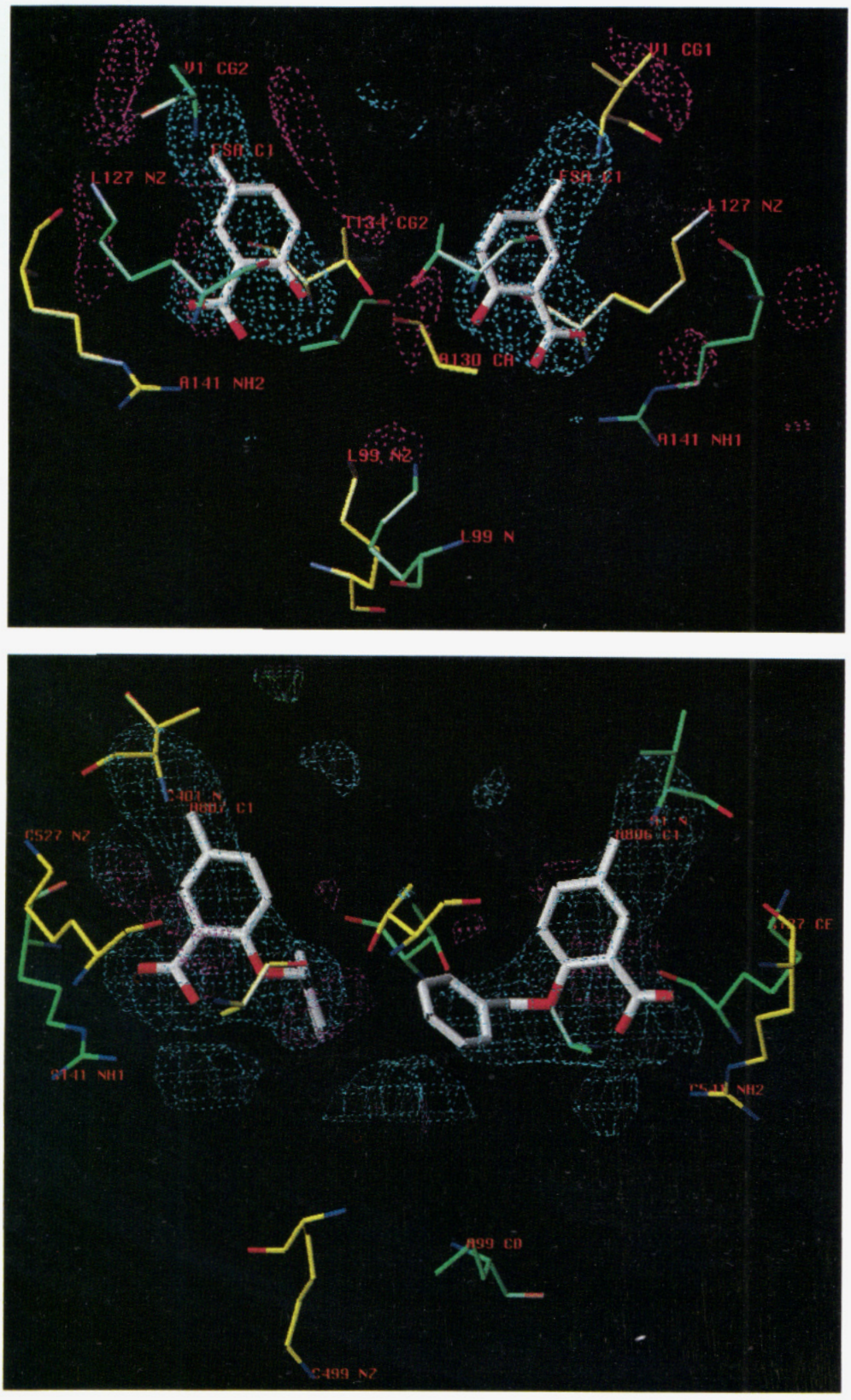

FIGURE 2: (a, top, left page) 5-FSA electron density confirmed the binding site as modeled in Figure 1a. The upper left 5-FSA is bound to Val $1\alpha_1$ (green) and the upper right to Val $1\alpha_2$ (yellow). There are positive (cyan) and/or negative (magenta) peaks found on or around the following globin residues, Val 1α, Arg 141α, Thr 134α, Lys 127α, Ala 130α, and Ser 131α, indicating minor Hb residue movements. The salt bridges between the carboxylate of 5-FSA and Arg 141α of the opposite subunit (yellow on the left and green on the right) add T-state constraint that results in a right shift of the oxygen equilibrium curve. The map was contoured at 3.5σ. (b, bottom, left page) Fitting of 2-BF (molecules in white) with the electron density overlapping the N-terminal nitrogens. Positive contours are in cyan and negative contours are in magenta. The α_1 residues are in green and the α_2 residues are in yellow. The density indicates that 2-BF binds nearer to Arg 141α than 5-FSA and its terminal phenyl ring is oriented toward Lys 99α of the opposite subunit deeper in the water channel. The phenyl carbons are 3.0−3.9 Å from Thr 137α, and the side-chain hydroxyl of this residue hydrogen bonds with the 2-BF phenyl ring

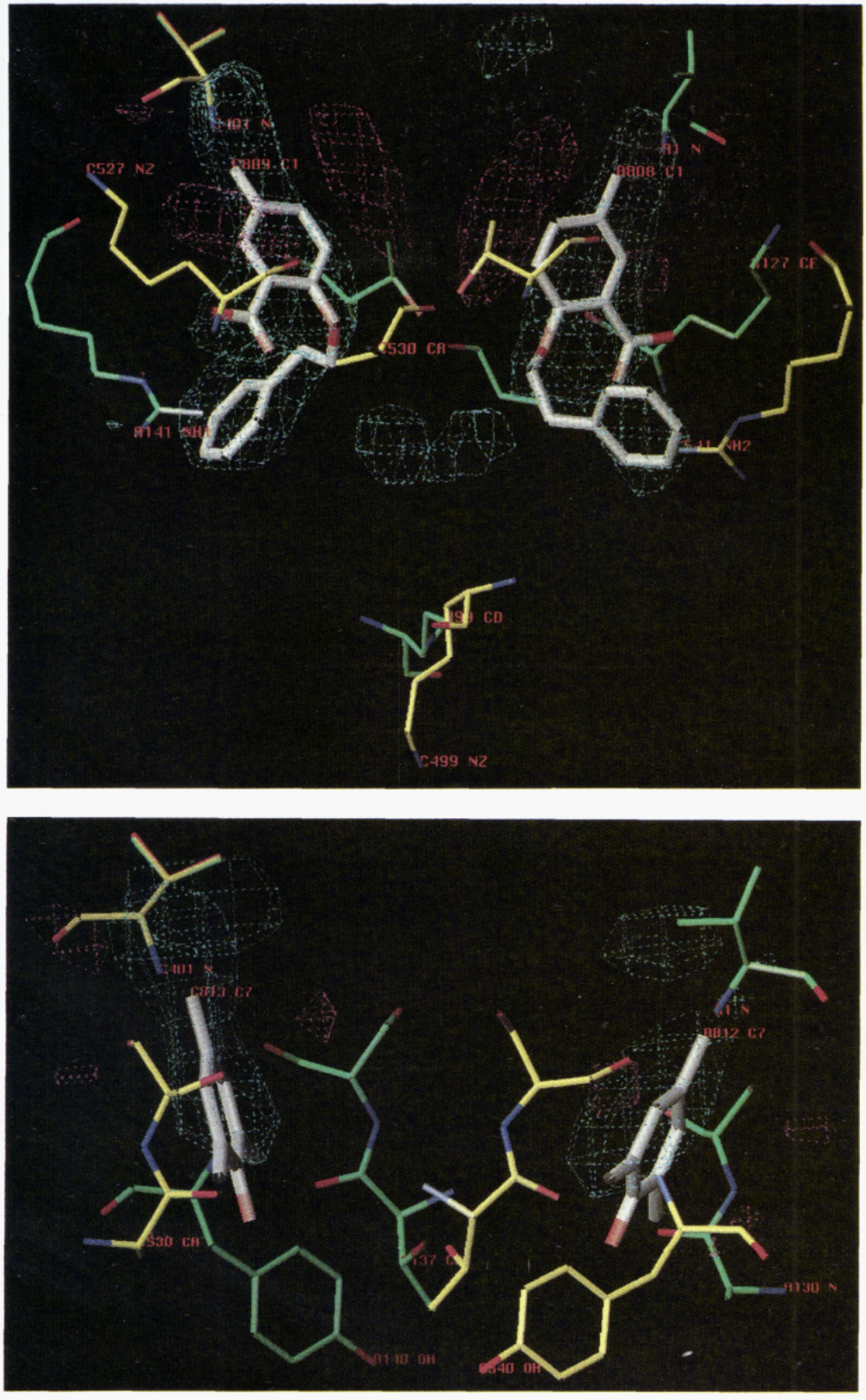

π electrons similar to the hydrogen bond found with the phenyl ring of noncovalent acting allosteric effectors (Wireko et al., 1991). The map was contoured at 3.0σ. (c, top, right page) This shows the fit of symmetry-related pairs of 2-PEF molecules (white) to the electron density. The α_1 residues are in green and the α_2 residues are in yellow. Positive contours are in cyan while negative ones are in magenta. 2-PEF is a carbon atom longer than 2-BF, and its phenyl ring is positioned even further down the water cavity than that of 2-BF. The map was contoured at 4.0σ. (d, bottom, right page) Electron density difference map of DMHB (white) showing binding to the N-terminal nitrogen atoms of Val 1α. Positive contours are in cyan while negative ones are in magenta. The α_1 residues are in green and the α_2 residues are in yellow. The hydroxyl group of DMHB is not involved in any cross-subunit interactions, and unlike 5-FSA and the other effectors that right shift the oxygen equilibrium curve, the aromatic ring is not in close contact with Arg 141α; however, it also is oriented down the central water cavity toward Lys 99α. This map was contoured at 4.0σ.

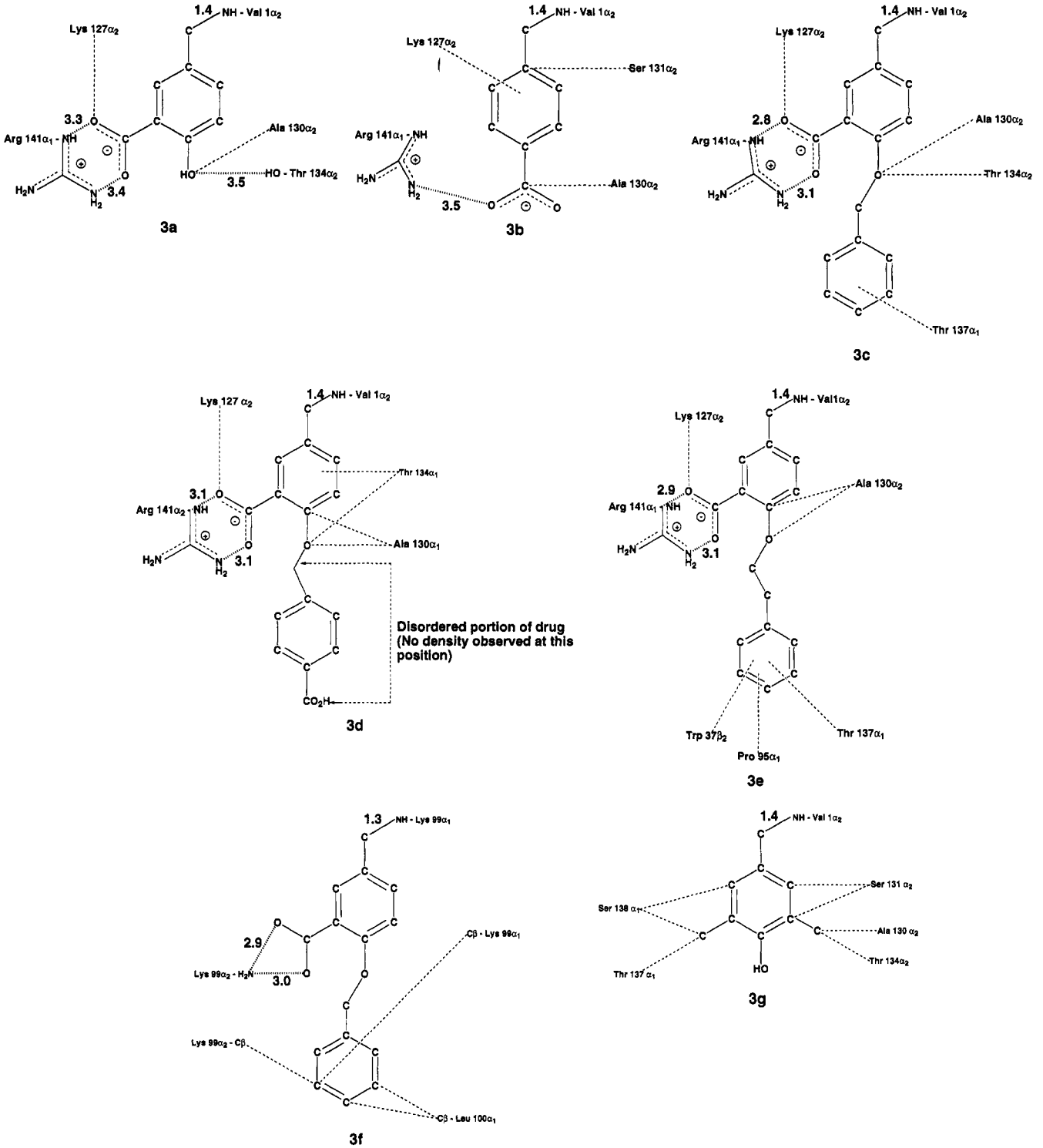

FIGURE 3: Close contacts within 4 Å and polar interactions of interest in angstroms: (3a) 5-FSA; (3b) 4-CBA; (3c) 2-BF; (3d) 2−4CBF; (3e) 2-PEF; (3f) 2-BF, second site bridging the Lys 99α residues; (3g) DMHB.

When Hb and 5-FSA were incubated and reduced under anaerobic conditions, four major binding sites were observed. The same two symmetry-related sites on the Val 1α N-terminal nitrogens were found with two symmetry-related binding sites on the Val 1β N-terminal nitrogens. The difference in degree of binding at the β subunits cleft is undoubtedly due to the larger pocket that is formed at the DPG site in deoxy-Hb (Arnone, 1972). DPG is the natural allosteric effector that binds to the β clefts predominantly in the T-state (Benesch et al., 1968).

(B) 4-Carboxybenzaldehyde (4-CBA). The electron density difference map indicated exclusive binding at the α subunit N-terminal amino atoms. The reduced Schiff base positions the acid group toward Arg 141α; however, only one carboxylate oxygen is able to make a hydrogen bond with the Arg 141 guanidinium ion as suggested in the modeling experiments. Positive and/or negative peaks are found on or around Val 1α, Thr 134α, Lys 127α, Ser 131α, Val 132α, and Arg 141α, indicating movements of these residues (Figure 3b).

(C) 5-Formylaspirin (5-FA). The electron density difference map indicated that the 5-FA acetate group had hydrolyzed and that the remainder of the molecule (5-FSA) was bound to the same site observed for 5-FSA (Figure 2). No definitive position was detected for the acetate group. Again, the shortest contact occurs between the β carbon of

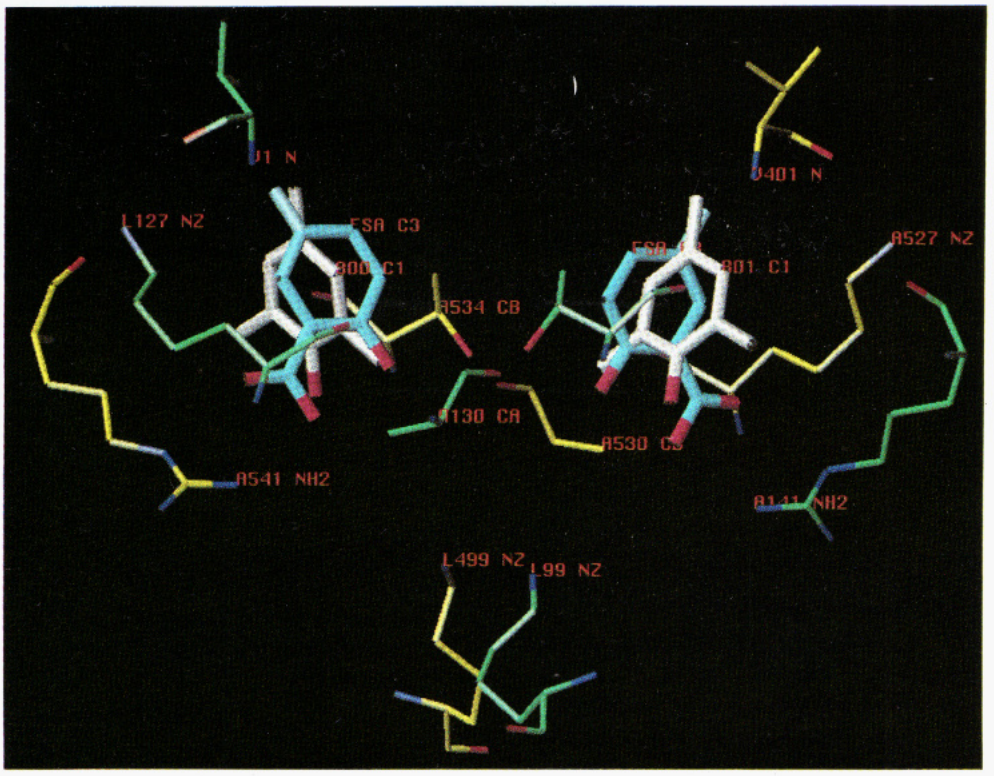

FIGURE 4: Superimposed binding sites for 5-FSA (blue) and DMHB (white). The α_1 subunits are in green and the α_2 subunits are in yellow. Both effectors are bound to Val 1α N-terminal amino groups. Note that the *para* position of 5-FSA points diagonally downward toward Lys 99α of the opposite subunit. The *m*-carboxylate forms a salt bridge interaction with Arg 141α, labeled A141 NH1, of the opposite subunit (middle left and right). The lack of a carboxylate on DMHB permits the aromatic ring to turn with no close contacts with the opposite subunit.

Ala 130α and the phenol oxygen of 5-FA, 2.9 Å. There are positive and/or negtive peaks found on or around the same globin residues as found on the binding of 5-FSA. Klotz et al. (1985) suggested from their experiments that 5-FA binds with oxy-Hb in the β cleft and reacts with the Lys 82β and Val 1β, but we see only weak binding at this site in the crystal structure (less than found for 5-FSA at the same sites).

(D) 2-(Benzyloxy)-5-formylbenzoic Acid (2-BF), 2-(Phenylethyloxy)-5-formylbenzoic Acid (2-PEF), and 2-(4-Carboxybenzyloxy)-5-formylbenzoic Acid (2−4CBF). The difference electron density maps for 2-BF (Figure 2b) and 2-PEF (Figure 2c) were well defined with the phenyl ring oriented as proposed toward Lys 99α. The 2−4CBF phenyl ring with the carboxyl group was disordered and could not be located (Figure 3d). The same bidentate salt bridge hydrogen bond network was observed between the carboxylate oxygen of 2-BF and 2-PEF and the Arg 141α guanidinium ion. The density indicates that 2-BF and 2-PEF bind nearer to Arg 141α than 5-FSA or 5-FA.

The 2-BF phenyl group is oriented toward Lys 99α of the opposite subunit deeper in the water channel. The phenyl carbons are 3.0−3.9 Å from Thr 137α (Figures 2b and 3c). The Thr 137α hydroxyl hydrogen bond with the phenyl ring π electrons is reminiscent of a similar interaction found between the Asn 108β amide hydrogen bond with the π-electron cloud of the terminal aromatic ring of the potent noncovalent allosteric effectors that reduce Hb oxygen affinity (Perutz et al., 1986; Abraham et al., 1992a). Again, the bond distance between the ether oxygen of 2-BF and β carbon of Ala 130α is short (3.2 Å). Positive and negative difference density indicates the same protein movements observed with 5-FSA and the other aldehydes.

An extra site was observed for 2-BF adjacent to both Lys 99α amino groups at about 30% relative occupancy to the primary site. The difference density indicated that two disordered molecules (Figure 3f) were bound with one orientation forming a Schiff base with one Lys 99α, while the carboxylate interacts with the symmetry-related Lys. In this orientation the unsubstituted phenyl ring is pointed down the central water cavity toward the β subunit cleft. The other orientation reversed the Schiff base and carboxylate interaction with the unsubstituted phenyl ring pointed up the central water cavity toward the α subunit cleft.

2-PEF is a carbon longer than 2-BF and positions its phenyl ring further down the central water channel. The phenyl ring carbons are 3.7−3.9 Å from Thr 137α and 3.2−4.0 Å from Pro 95α (Figures 2c and 3e). The shortest aldehyde ether oxygen and Ala 130α β carbon contact is 3.2 Å. The same movements of protein residues were observed. No additional drug binding site was observed for 2-PEF.

(E) 3,5-Dimethyl-4-hydroxybenzaldehyde (DMHB). As suspected, DMHB is oriented differently than the other aldehydes. The electron density difference map does show exclusive binding to the N-terminal amino atoms of Val 1α, and the hydroxide is not involved in any apparent interactions (Figures 2d and 3g). There are nonbonded interactions between the methyl groups and the residues Ser 138α, Ser 131α, Ala 130α, and Thr 137α. Positive and/or negative peaks indicating Hb residue movements were found on or around globin residues Val 1α, Lys 127α, Ser 131α, Val 132α, and Arg 141α. Unlike 5-FSA and the other aldehydes, the aromatic ring is not oriented toward or in close contact with Arg 141α but still pointed down the central water cavity toward Lys 99α (Figure 4).

Oxygen Equilibrium Studies. Oxygen binding curves were performed on solutions obtained from T-state crystals so that accurate parameters could be measured on purified effector−

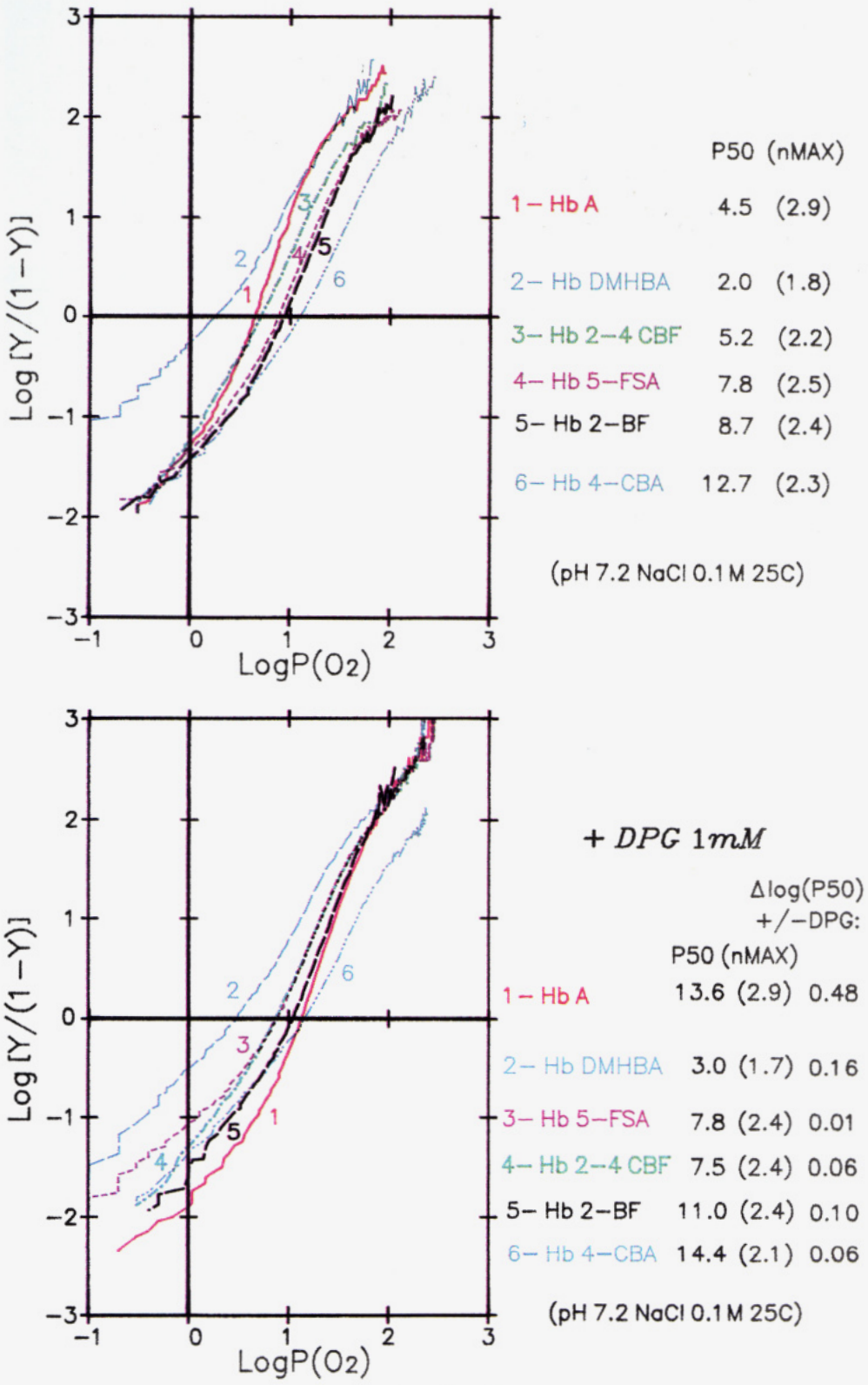

FIGURE 5: Hill plots made from the oxygen binding curves of solutions from T-state Hb crystals used in the diffraction studies. Experimental conditions were without (a, top) and with (b, bottom) addition of 1 mM NaDPG. The P_{50} values are listed to the right with the maximal Hill coefficients (n_{max}).

Hb complexes and on the same material used to identify the binding sites. Linking structure/function studies by using the same material is important since the degree of reaction in solution can vary dramatically depending on the ratio of reactant/protein and on the allosteric state of the protein.

The effect of the monoaldehydes on the affinity of hemoglobin for oxygen in solutions obtained from the crystals is shown in Figure 5a. Four of the monoaldehydes exhibited moderate right shifts producing low-affinity hemoglobins. The order of degree of shift in P_{50} increases starting with 2–4CBF, 5-FSA, 2-BF, and 4-CBA. It is important to note that, in spite of varying increases in P_{50} values, all four effectors display an almost constant lower asymptote (K_T) while exhibiting low n_{max} values relative to native Hb. K_T is the equilibrium constant for the deoxy (T) state.

Table 2: Allosteric Parameters for Monoaldehyde Allosteric Effector−HbA Complexes[a]

monoaldehyde effector−HbA complexes	P_{50}, mmHg	n_{50}	L^b	c^c	K_R, mmHg	K_T, mmHg	% $T_3{}^d$	$i_s{}^e$	$\sigma^f \times 10^3$
HbA	4.5	2.8	$1e^5$	0.0097	0.24	24.7	8	2.48	6.1
Hb−2−4CBF	5.2	2.2	$2.1e^4$	0.0220	0.4	18.2	18	2.61	8.0
Hb−2-BF	8.7	2.4	$1.6e^5$	0.0140	0.4	28.6	31	2.81	5.2
Hb−4-CBA	12.7	2.3	$2.8e^5$	0.0170	0.5	29.4	57	3.08	6.8

[a] Conditions: pH 7.2, 0.1 M NaCl, 0.05 M bis-Tris, 50 μM EDTA, 20 μg/mL catalase, [heme] = 60−70 μM, 25 °C. [b] $L = T_0/R_0$. [c] $c = K_R/K_T$. [d] % $T_3 = (Lc^3)/(1 + Lc^3)$. [e] $i_s = -\log L/\log c$. [f] σ = standard error by point.

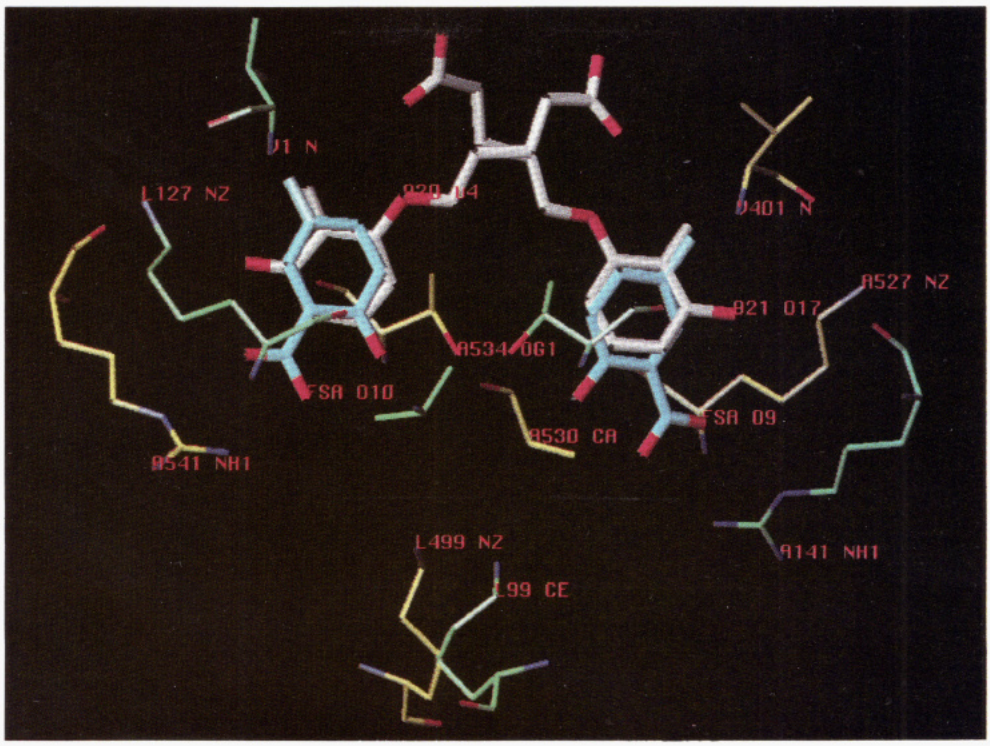

FIGURE 6: Superimposed binding modes of 5-FSA (blue) and 12C79 (white). The α_1 subunits are in green and the α_2 subunits are in yellow. Both effectors are bound to Val 1α N-terminal amino groups. Note that the *para* position of 5-FSA points diagonally downward toward Lys 99α of the opposite subunit. The *m*-carboxylate forms a salt bridge interaction with Arg 141α, labeled A141 NH1, of the opposite subunit (middle left and right). 12C79 points its acid chain diagonally upward (toward the center) and does not form any contacts with any residues on the opposite α chains.

DMHB was the only monoaldehyde to produce a high-affinity hemoglobin that left shifts the curve. Remarkably, this curve has a diminished n_{max} value of 1.8 while the upper asymptote [K_R, equilibrium constant for oxy (R) state] is superimposed over the native Hb curve.

Figure 5b illustrates the oxygen equilibrium curves for these effectors in the presence of 1 mM DPG. The last column shows that the interaction of DPG with the Hb complexes (Δ log P_{50} ± DPG) is either diminished or abolished. This leads to a left shift in the oxygen equilibrium curves relative to native Hb in the presence of DPG. Note that DMHB differs from the other effectors as it retains about one-third of the normal DPG effect. A large inhibition of the oxygen-linked chloride effect and a normal alkaline Bohr effect for compounds 2-BF and DMHB were observed (C. Poyart, J. Kister, and D. J. Abraham, manuscript in preparation).

The allosteric constants for the derivatized hemoglobins were determined from the oxygen binding curves using the MWC model (Monod et al., 1965) and are listed in Table 2. The derivatives that lower Hb oxygen affinity exhibited a significant increase in K_T (binding constant to the T-state) together with a significant increase in the allosteric equilibrium constant (L). As expected for the monoaldehydes in this study, the % T_3 (triligated T-state Hb) and the switchover points (i_s) are not as great as those determined for the derivatized hemoglobins that covalently cross-link the dimer interface as observed with the bisaldehydes in the accompanying study (Boyiri et al., 1995). We cannot separate out the effect on the oxygen binding curves of binding of the monoaldehydes to a portion of the β subunit N-terminal Val 1 residues. The fact that the oxygen binding studies follow the MWC model supports the conclusion that the P_{50} values observed correspond to the major fractions in the electrophoresis which in turn correspond to the agreement between the observed X-ray binding sites and the sequencing results.

The increase in K_T and L (for the derivatives that lower Hb oxygen affinity) is consistent with the interpretation that they place a greater constraint on the T-state as proposed below, as demonstrated in the accompanying paper (Boyiri et al., 1995) and as found in our other studies with noncovalent-acting allosteric effectors (Abraham et al., 1995).

DISCUSSION

Beddel et al. (1984) designed three different classes of substituted benzaldehydes that would interact preferentially with the α subunit N-terminal amino group in the R-state. Molecules from all three classes and salicylaldehyde were shown to *left shift* the oxygen equilibrium curve and produce

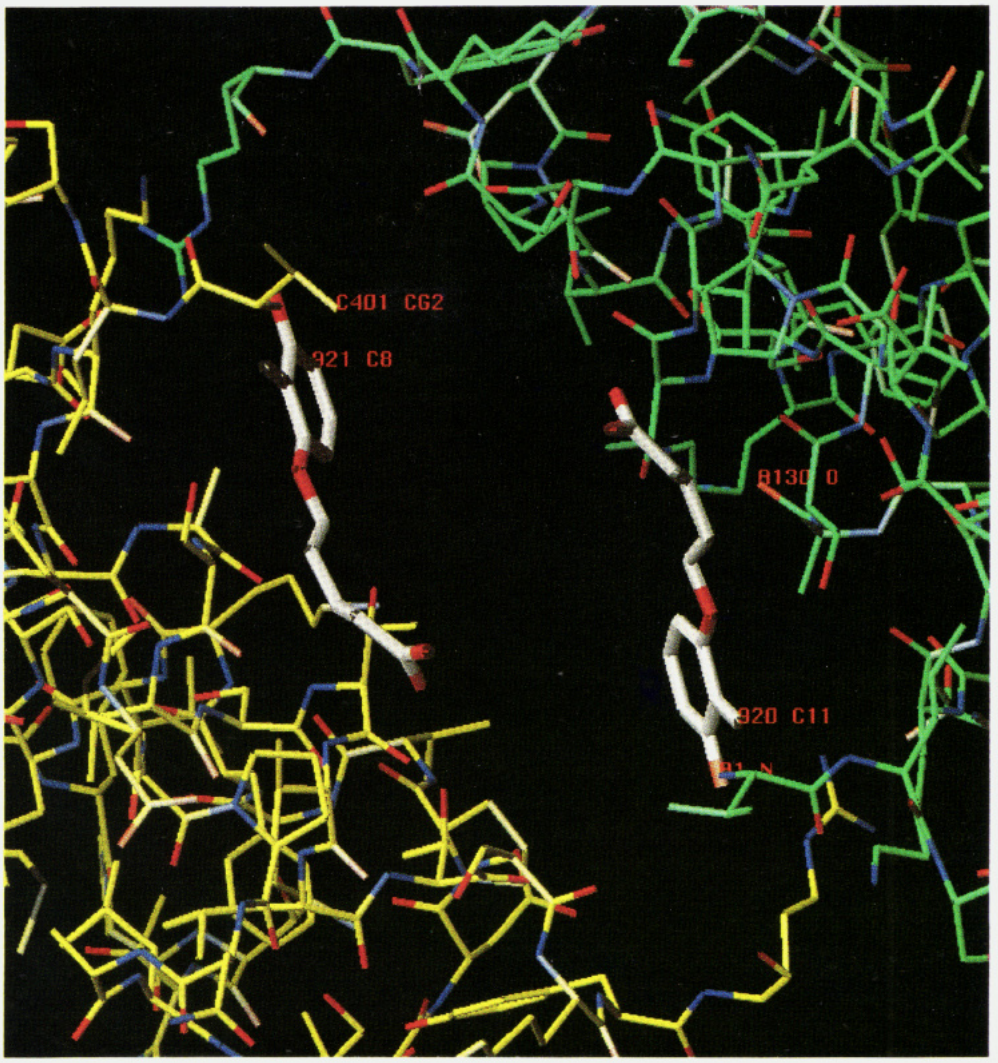

FIGURE 7: Top of the central water cavity with two molecules of 12C79 bound to the N-terminal Val residues. The α_1 subunits are in green and the α_2 subunits are in yellow. 12C79 (white) makes no cross-subunit interactions. It is proposed that the occupancy of the 12C79 molecules in the central water cavity will break the proposed water or weak salt bridge interaction between the α chain termini as well as reduce access of chloride ions to the central water cavity. The combination of no cross-subunit interactions, disruption of T-state bridges, and reduction of the chloride effect results in a left shift of the oxygen equilibrium curve.

high-affinity hemoglobins. Merrett et al. (1986) studied one of these aldehydes (12C79) with a ^{14}C-radiolabeled formyl group. Radiolabeled 12C79, when incubated in the R-state, reacted primarily at the α chains while incubation under T-state conditions produced radiolabels on both the α and β chains. We later confirmed (Wireko & Abraham, 1991) that 12C79 had covalently bound to Val 1α in T-state crystals. However, 12C79 was not oriented horizontally across the molecular 2-fold axis in T-state crystals, but the aromatic ring with its extended acid chain pointed upward and diagonally along the cavity wall toward the opening of the α subunit central water cavity (Figure 6).

To our surprise, the aromatic aldehydes chosen for this study that also contain an acid group and bind to Val 1α exhibit a *right shift* in the oxygen curve to produce low-affinity hemoglobins. DMHB, on the other hand, does not contain an acid group and produces a *left shift*. We asked the question, how can allosteric effectors of similar structure bind to the same amino acid residue yet produce opposite allosteric effects? In order to answer this question, the focus of our attention was turned toward the X-ray crystallographically determined binding sites of the allosteric effectors and the surrounding environment near the N-terminal Val 1 residues on the α chains.

The N-terminal Val 1α nitrogen was originally reported at low resolution (3.5 and 5 Å) to possibly form a salt bridge with the C-terminal carboxylate of Arg 141α (Muirhead & Greer, 1970; Muirhead et al., 1967). Fermi refined the three-dimensional human deoxyhemoglobin structure to 2.5 Å (Fermi, 1975) and then 1.7 Å (Fermi et al., 1984) and found these groups to be too far apart for a salt bridge (5.3 and 4.6 Å, respectively). Fermi stated that, in view of the evidence for the involvement of the terminal amino group of the α chain in the Bohr effect, it appears likely that the amino and carboxyl termini of the opposite α chains of deoxyhemoglobin are involved in some form of linkage, perhaps mediated by a water molecule, that is broken upon oxygenation to the R-state (Fermi, 1975). The salt bridge charge attraction, even at 4.6 Å, may be sufficiently effective to orient the residues to the positions found in the electron density. We checked this by estimating the strength of this interaction using the 1.7 Å T-state coordinates (Fermi et al., 1984) and HINT, a computational software package developed in our laboratory to visualize and estimate *h*ydropathic *int*eractions (Wireko et al., 1991; Kellogg et al., 1992). HINT interaction scores indicated a significant attraction at 4.6 Å between the N-terminal amino group and the C-terminal carboxylate. The good interaction score was due

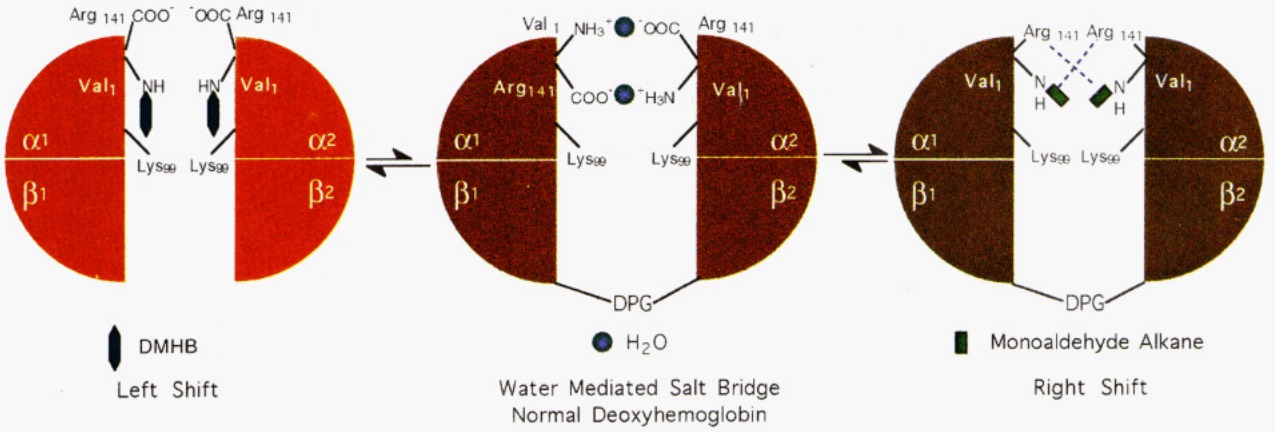

FIGURE 8: Summary of the proposed hypothesis to explain the opposite allosteric effects demonstrated by similar aldehyde acids that bind to Val 1α. Fermi (1975) has proposed that it appears likely that the amino and carboxyl termini of the opposite α chains of deoxyhemoglobin are involved in some form of linkage, perhaps mediated by a water molecule, that is broken upon oxygenation to the R-state. This is shown in the central diagram and depicts the normal constraint of the T-state. Also possible is the stabilization of T-state Hb (center) by an anion binding site linking the N-terminal amino group of Val 1α with the guanidinium ion of Arg 141α of the opposite subunit (O'Donnell et al., 1979; Nigen et al., 1980). When DPG, the natural allosteric effector, is bound to the bottom of the central water cavity adding extra constraint to the T-state by tying together the β subunits, the oxygen equilibrium is shifted to the right. When the allosteric monoaldehyde effectors (except DMHB) are reacted with Hb, they add further constraint to the T-state by forming intersubunit salt bridges with Arg 141α (diagram on the right). This combination of bonds and interactions provides a shift of the oxygen equilibrium to the right and produces a hemoglobin with low affinity for oxygen. On the other hand, effectors that left shift the oxygen equilibrium curve to produce high-affinity hemoglobins bind to Val 1α with no intersubunit T-state interactions, narrow the central water cavity inhibiting nonspecific chloride binding (Perutz et al., 1993), and disrupt the T-state salt, anion binding, and/or proposed water-mediated bridge between the opposing termini of the α chains. This is depicted in the left-hand diagram with the allosteric effector DMHB.

to idealized positions of the charged groups with little negative interactions between the charges and nonpolar atoms.

Perutz et al. (1994) recently reexamined the high-resolution R-state oxyhemoglobin crystal structure and observed that no density is observed for Val 1α or Lys 82β. They concluded that these basic amino acids are mobile and may not contribute to the paucity of positive charges in the central water cavity. Therefore, it appears clear that in the T to R transition, Val 1α proceeds from a more restricted state to a more mobile state, thereby releasing some T-state constraint. The more disordered environment in oxy-Hb around the N-terminal nitrogen provides a structural explanation for the lowering of its pK_a and release of Bohr protons (Kilmartin & Rossi-Bernardi, 1973).

The results from the studies described above enable us to propose a hypothesis that may answer the question of how allosteric effectors can bind to the same protein residue and produce opposite shifts in the allosteric equilibrium.

Aldehydes such as DMHB and 12C79 that *left shift* the oxygen equilibrium curve *add no new cross-subunit interactions* and disrupt any T-state salt- or water-bridged interactions between the opposing α chains. In this regard, binding to Val 1α by such an allosteric effector could also disrupt an observed anion bridge between Val 1α and the guanidinium ion of Arg 141α of the opposite subunit (O'Donnell et al., 1979) to destabilize the T-state structure. Possibly more important is that they may also reduce the positive charge in the central water cavity and retard the entrance of small anion allosteric effectors such as chloride into the central water cavity. The role of small anion allosteric effectors of hemoglobin that bind to the central water cavity has been previously addressed (Fronticelli et al., 1988; Ueno & Manning, 1992; O'Donnell et al., 1979). As demonstrated by Nigen et al. (1980) for carbamylation of the α chains, we also found little or no effect on P_{50} by addition of low chloride ion concentrations.

Perutz et al. (1994) have suggested a new kind of allosteric mechanism for the chloride effect in human Hb. Chloride ion is an allosteric effector of mammalian hemoglobin that stabilizes the T-state and reduces the oxygen affinity as demonstrated by a right shift in the oxygen equilibrium curve. Perutz et al. (1993) have proposed that the chloride effect may not be due to specific binding to any residues (as thought earlier) but is due to the widening of the central water cavity that allows additional chloride to diffuse in to neutralize the excess positive charges that line the central water cavity. Agents such as DMHB and 12C79 (Figure 7) would narrow the access to the central water cavity and retard by steric principles some of the chloride effect. Also important is the fact that most of the effectors studied here and those that are reported in the adjacent paper (Boyiri et al., 1995) contain carboxylates that would further retard chloride binding in the central water cavity. On the other hand, there is no reduction in charge in the central cavity by reaction of DMHB since the reduced Schiff base is a secondary amine. The absence of the chloride effect in this case may be due to the narrowing of the central water cavity. The retardation of the chloride effect, together with disruption of any terminal salt bridge or water-mediated interactions that link the two α subunits, should produce a left shift in the oxygen equilibrium curve, and that is what is observed experimentally.

Effectors such as 5-FSA, 2-BF, and 2−4CBF *right shift* the curve since the position of the carboxylate on the aromatic ring enables the formation of a tight salt bridge interaction across the α subunits with the guanidinium ion of Arg 141α (Figure 2) and add constraint to the T-state. Effectors such as DMHB *left shift* the oxygen equilibrium curve by destabilization of the T-state.

The hypothesis to explain the different allosteric properties produced by agents bound to the same amino acid residue is summarized in Figure 8. The allosteric equilibrium is primarily regulated by stabilization or destabilization of the

tense allosteric state (conformation). The R conformations are energetically relaxed states relative to the tense state conformation as we have recently shown by computational analysis of intersubunit interactions in T, R_1, and R_2 hemoglobins (Abraham, Kellogg, Holt, and Ackers, unpublished results).

The N-terminal Val residues on the α and β clefts have previously been shown to react in both the T- and R-states with a number of negatively charged chemical modifiers and cross-linking agents (Manning & Manning, 1988; Manning et al., 1991; Schumacher et al., 1995; Bonaventura & Bonaventura, 1978; Nigen et al., 1974; Kavanaugh et al., 1988). Detailed structural identification has been provided with a few of these agents (Schumacher et al., 1995; Fantl et al., 1987; Arnone, 1972). Bonaventura and Bonaventura (1978) have proposed that a reduction in the positive charge of the Hb central cavity, such as in acetylated Hb, reduces oxygen affinity.

To our knowledge, a structural correlation that details the interactions responsible for the difference in direction in shift of the oxygen equilibrium by agents bound to the same amino acid has not been made previously. In the accompanying paper, we further test this hypothesis by modifying the 5-FSA nucleus and extending a chain with a second reactive aldehyde to see if stronger constraints can be made on the T-state by cross-linking Lys 99α or Val 1α of the opposite subunit. Lys 99α has been shown to be an important residue in the regulation of the allosteric equilibrium toward the T-state (Wireko et al., 1991; Abraham et al., 1995).

ACKNOWLEDGMENT

This paper is dedicated to the 80th birthday celebration for Dr. Max F. Perutz held in London on Sept 23, 1994. The authors gratefully acknowledge discussions with Drs. Max Perutz, Eugene Orringer, Terry Jones, and Michael Channey and technical assistance by Mr. Mark Eaton (Richmond), Jayashree Panikker (Richmond), and Mrs. G. Caron (Paris).

REFERENCES

Abraham, D. J., Perutz, M. F., & Phillips, S. E. V. (1983) *Proc. Natl. Acad. Sci. U.S.A. 80*, 324.
Abraham, D. J., Mehanna, A. S., Wireko, F. C., Whitney, J., Thomas, R. P., & Orringer, E. P. (1991) *Blood 77*, 1334.
Abraham, D. J., Peascoe, R. A., Randad, R. S., & Panikker, J. (1992a) *J. Mol. Biol. 227*, 480.
Abraham, D. J., Wireko, F. C., Randad, R. S., Poyart, C., Kister, J., Bohn, B., Liard, J.-F., & Kunert, M. P. (1992b) *Biochemistry 31*, 9141.
Abraham, D. J., Kister, J., Joshi, G. S., Marden, M. C., & Poyart, C. (1995) *J. Mol. Biol. 248*, 845.
Arnone, A. (1972) *Nature 237*, 146.
Beddell, C. R., Goodford, P. J., Kneen, G., White, R. D., Wilkinson, S., & Wootton, R. (1984) *Br. J. Pharmacol. 82*, 397.
Benesch, R., Benesch, R. E., & Yu, C. I. (1968) *Proc. Natl. Acad. Sci. U.S.A. 59*, 526.
Bonaventura, C., & Bonaventura, J. (1978) in *Biochemical and Clinical Aspects of Hemoglobin Abnormalities* (Caughey, W. S., & Caughey, H., Eds.) pp 647−663, Academic, New York.
Boyiri, T., Safo, M. K., Danso-Danquah, R. E., Kister, J., Poyart, C., & Abraham, D. J. (1995) *Biochemistry 34*, 15021−15036.
Currell, D. L., Nguyen, D. M., Ng, S., & Hom, M. (1982) *Biochem. Biophys. Res. Commun. 106*, 1325.
Evans, P. (1985) *Med. Res. Counc. Lab. Mol. Biol.*, Cambridge, U.K.
Fantl, W. J., Di Donato, A., Manning, J. M., Rogers, P. H., & Arnone, A. (1987) *J. Biol. Chem. 262*, 12700.
Fermi, G. (1975) *J. Mol. Biol. 97*, 237.
Fermi, G., Perutz, M. F., Shaanan, B., & Fourme, R. (1984) *J. Mol. Biol. 175*, 159.
Fronticelli, C., Bucci, E., & Razynska, A. (1988) *J. Mol. Biol. 202*, 343.
Goodford, P. J. (1985) *J. Med. Chem. 28*, 849.
Kavanaugh, M. P., Shih, D. T.-B., & Jones, R. T. (1988) *Biochemistry 27*, 1804.
Kellogg, G. E., Joshi, G. S., & Abraham, D. J. (1992) *Med. Chem. Res. 1*, 444.
Kilmartin, J. V., & Rossi-Bernardi, L. (1973) *Physiol. Rev. 53*, 836.
Kister, J., Poyart, C., & Edelstein, S. J. (1987) *J. Biol. Chem. 262*, 12085.
Manning, L. R., & Manning, J. M. (1988) *Biochemistry 27*, 6640.
Manning, L. R., Morgan, S., Beavis, R. C., Chait, B. T., Manning, J. M., Hess, J. R., Cross, M., Currell, D. L., Marini, M. A., & Winslow, R. M. (1991) *Proc. Natl. Acad. Sci. U.S.A. 88*, 3329.
Merrett, M., Stammers, D. K., White, R. D., Wootton, R., & Kneen, G. (1986) *Biochem. J. 239*, 387.
Monod, J., Wyman, J., & Changeux, J. (1965) *J. Mol. Biol. 12*, 88.
Muirhead, H., & Greer, J. (1970) *Nature 228*, 516.
Muirhead, H., Cox, J. M., Mazzarella, L., & Perutz, M. F. (1967) *J. Mol. Biol. 28*, 117.
Nigen, A. M., Njikam, N., Lee, C. K., & Manning, J. M. (1974) *J. Biol. Chem. 249*, 6611.
Nigen, A. M., Manning, J. M., & Alben, J. O. (1980) *J. Biol. Chem. 255*, 5525.
O'Donnell, S., Mandaro, R., Shuster, T. M., & Arnone, A. (1979) *J. Biol. Chem. 254*, 12204.
Orringer, E. P., Binder, E. A., Thomas, R. P., Blythe, D. S., Bustrack, J. A., Schroeder, D. H., & Hinton, M. L. (1988) *Blood 72*, 69a.
Perutz, M. F. (1968) *J. Cryst. Growth 2*, 54.
Perutz, M. F., Fermi, G., Abraham, D. J., Poyart, C., & Bursaux, E. (1986) *J. Am. Chem. Soc. 108*, 1064.
Perutz, M. F., Fermi, G., Poyart, C., Pagnier, J., & Kister, J. (1993) *J. Mol. Biol. 233*, 536.
Perutz, M. F., Shih, D. T. B., & Williamson, D. (1994) *J. Mol. Biol. 239*, 555.
Schumacher, M. A., Dixon, M. M., Kluger, R., Jones, R. T., & Brennan, R. G. (1995) *Nature 375*. 84.
Still, W. C., Mohamadi, F., Richards, N. G. J., Guida, W. C., Lipton, M., Liskamp, R., Chang, G., Hendrickson, T., Degunst, F., & Hasel, W. (1989) in *MACROMODEL*, Department of Chemistry, Columbia University, New York.
Ueno, H., & Manning, J. M. (1992) *J. Protein Chem. 11*, 177.
Wireko, F. C., Kellogg, G. E., & Abraham, D. J. (1991) *J. Med. Chem. 34*, 758.
Wireko, F. C., & Abraham, D. J. (1991) *Proc. Natl. Acad. Sci. U.S.A.* 88, 2209.

BI950434K